Journal of Optoelectronics and Advanced Materials Vol. 6, No. 3, September 2004, p. 737 - 746

PHYSICAL PROPERTIES OF PbO-ZnO-P_2O_5 GLASSES I. INFRARED AND RAMAN SPECTRA

J. Schwarz, H. Tichá*, L. Tichý[a], R. Mertens

University of Pardubice, Faculty of Chemical Technology, 532 10 Pardubice, Czech Republic
[a]Joint Laboratory of Solid State Chemistry of the Institute of Macromolecular Chemistry of the Academy of Sciences of the Czech Republic and the University of Pardubice, 532 10 Pardubice, Czech Republic
[c]RUCA, University of Antwerp, B-2020 Antwerp, Belgium

Phosphate glasses of composition x PbO – 10 ZnO - (90-x) P_2O_5, 30 ≤ x(mol. %) ≤ 55 (series A); 50 PbO –x ZnO – (50-x) P_2O_5, 0 ≤ x(mol %) ≤ 20 (series B); and x PbO – (60 – x) ZnO - 40 P_2O_5, 0 ≤ x(mol %) ≤ 60 (series C), were investigated. Depending mainly on the PbO content in glasses, the density varies in the range 3.2 to 5.5 [g/cm^3], the glass-transition temperature lies in the region 270 – 394 °C. Both the Raman and infrared spectroscopy were used to study the considerable structural changes in the phosphate network induced by incorporation of PbO and ZnO into a glass network. Depending on the actual system, PbO behaves as a network modifier and/or network former, especially for higher content of PbO. ZnO in most of cases seems to prefer to interact with PO_3-end groups. In the C-series of glasses the local minimum in the glass-transition temperature T_g(PbO) dependence, we speculate, could reflect some tendency of the system to a local nano-phase separation.

(Received April 27, 2004; accepted June 22, 2004)

Keywords: Phosphate glasses, glass-transition temperature, infrared spectroscopy, Raman spectroscopy

1. Introduction

The lead zinc phosphate glasses are known as materials considered for nuclear wastes storage [1], and owing to their low glass-transition temperature and suitable high thermal expansion coefficients, they are also interesting for some sealing applications [2]. In the last years various properties of PbO-ZnO-P_2O_5 glasses were studied and some main results can be summarized as follows:

(a) The glass-transition temperature varies in the region 280–380 °C [3];

(b) The chemical durability, measured by a dissolution rate of a glass in deionised water is comparable to that of standard window glasses for the content of P_2O_5 equal or less to 40 mol. % [3];

(c) The glasses are colourless [4] and for example in the system $(PbO)_x(ZnO)_{0.6-x}(P_2O_5)_{0.4}$ the refractive index (n) can be taylored from the value n = 1.57 (x=0) to n = 1.83 (x=0.6) [5].

The structure of PbO-ZnO-P_2O_5 glasses was studied using various techniques, e.g. the infrared and Raman spectroscopy, the nuclear magnetic resonance [2,5], and X-Ray photoelectron spectroscopy [3]. From the results published it follows, that e.g. in ultraphosphate glasses ([P_2O_5] > 50 mol. %) both, the PbO and ZnO enter the network mainly as modifiers [2]. The further lowering of P_2O_5 content to metaphosphates ([P_2O_5] = 50 mol. %) and namely up to polyphosphates ([P_2O_5] < 50 mol. %) is associated with the formation of covalent P–O–Pb(Zn) linkages, which give rise to an increase of connectivity and the cross-linking of the network. Hence, T_g increases and

* Corresponding author: helena.ticha@upce.cz

stability to water corrosion increases, too [3]. In polyphosphate glasses, where $[P_2O_5]$ = 40 mol. %, however, ZnO has a role of network modifier while the Pb-atoms have a mixed role of both, the network former and network modifier. Hence, the value of T_g decreases with PbO increase [5].

In this communication the basic physical properties, i.e. the density (ρ), the molar volume (V_m), and the glass-transition temperature (T_g), are put together with the results of study of both the Raman (R) and infrared (IR) spectra of all studied glasses. The results obtained are discussed in relation to the compositional dependencies of properties studied.

2. Experimental

The studied glasses of PbO-ZnO-P_2O_5 system, see Table 1, were prepared from oxides PbO, ZnO (purity > 97 %, Aldrich), and H_3PO_4 (85 %, p.a., Lachema Brno, Czech Republic) in Pt-crucible. The stoichiometric amounts of oxides and H_3PO_4 (diluted by distilled water) were mixed and heated for approximately 3 hours up to the temperature T ~ 500 °C. In the next step the heating and melting of obtained oxides at T ~ 1050 °C for about 20 min was done. Then the melt was poured onto a polished nickel plate at room temperature and glassy (confirmed by the absence of XRD patterns), colourless and transparent samples were obtained.

The density (ρ) of the glasses was determined using the standard Archimedean method. The molar volume (V_m) was calculated according to relation: $V_m = \overline{M}/\rho$, where $\overline{M}$ is the average molar weight of the glass.

The values of the dilatometric glass-transition temperature (T_g) were estimated from thermomechanical analysis of the samples. The cubes of glasses 5x5x5 mm were heated (the heating rate of 5 K min^{-1}) in the TMA CX04 equipment (R.M.I. Pardubice, Czech Republic) and from the thermal expansion curves using the slope intercept method the values of T_g were determined.

The Raman spectra were measured at room temperature on bulk samples with FTIR spectrometer, Bruker model IFS 55 (Raman attachment FRA 106, Nd:YAG laser radiation, resolution of 4 cm^{-1}, power on the sample of 300 mW and 200 scans, resp.).

The MID infrared spectra were measured using the FTIR Thermo Nicolet Nexus spectrophotometer on the bulk optically polished samples

3. Results

3.1. Glass preparation and some basic physical parameters

Sixteen glasses from the PbO-ZnO-P_2O_5 system [6] were prepared and investigated. By chemical composition the glasses studied can be divided into three compositional series:

Series A, x PbO - 10 ZnO – (90-x) P_2O_5, $30 \leq x \leq 55$;

Series B, 50 PbO - x ZnO – (50-x) P_2O_5, $0 \leq x \leq 20$;

Series C, x PbO – (60–x) ZnO - 40 P_2O_5, $0 \leq x \leq 60$.

In Table 1 are summarized the chemical composition (in mol. %), the values of the density (ρ), the average molar volume (V_m), and the dilatometric glass-transition temperature (T_g), for all prepared glasses. As evident from Table 1, e.g. the values of the glass-transition temperatures are in the region $270 \leq T_g\,[°C] \leq 394$, and they scale roughly inversely to the molar volume.

3.2. Raman and infrared spectroscopy

It is well known that the phosphate network is built up from corner-sharing PO_4 tetrahedral units. According to the number of bridging oxygens the tetrahedral units are usually classified according to their connectivity (Q^n [7]), where n (n = 0, 1, 2, 3) is the number of bridging oxygens per PO_4 tetrahedron. Consequently, the Raman and infrared response of a phosphate network can roughly be divided into the three spectral regions related to the activity of: (i) non-bridging oxygen

modes, $\nu \sim 940 - 1380$ cm^{-1}; (ii) bridging oxygen modes, $\nu \sim 700 - 900$ cm^{-1}; (iii) deformation modes, $\nu \sim 500$ cm^{-1}, resp.

Table 1. Number of the sample (No(series)), the chemical composition, the density (ρ), the molar volume (V_m), the glass transition temperature (T_g), of glasses studied. By asterisk (*) is marked the joint composition for all three series.

No (series)	Chem. composition [mol %]			ρ [g/cm^3]	V_m [cm^3/mol]	T_g [°C]
	PbO	ZnO	P_2O_5			
1(A)	30	10	60	3.74	42.81	270
2(A)	35	10	55	3.99	41.18	273
3(A)	40	10	50	4.31	39.10	320
4(A)	45	10	45	4.68	36.87	325
5(A,B,C)*	50	10	40	5.10	34.61	344
6(A)	55	10	35	5.50	32.82	359
7(B)	50	0	50	4.64	39.35	287
8(B)	50	5	45	4.86	36.94	321
5(A,B,C)*	50	10	40	5.10	34.61	344
9(B)	50	15	35	5.41	32.07	359
10(B)	50	20	30	5.60	30.44	370
11(C)	60	0	40	5.37	35.48	345
5(A,B,C)*	50	10	40	5.10	34.61	344
12(C)	40	20	40	4.63	35.08	329
13(C)	30	30	40	4.47	33.13	347
14(C)	20	40	40	4.01	33.38	354
15(C)	10	50	40	3.55	33.71	360
16(C)	0	60	40	3.20	33.05	394

In Figs. 1a, 2a, 3a, the Raman spectra, and in Figs. 1b, 2b, 3b, the infrared spectra (in absorbance vs. wave number) are shown, for the studied glasses.

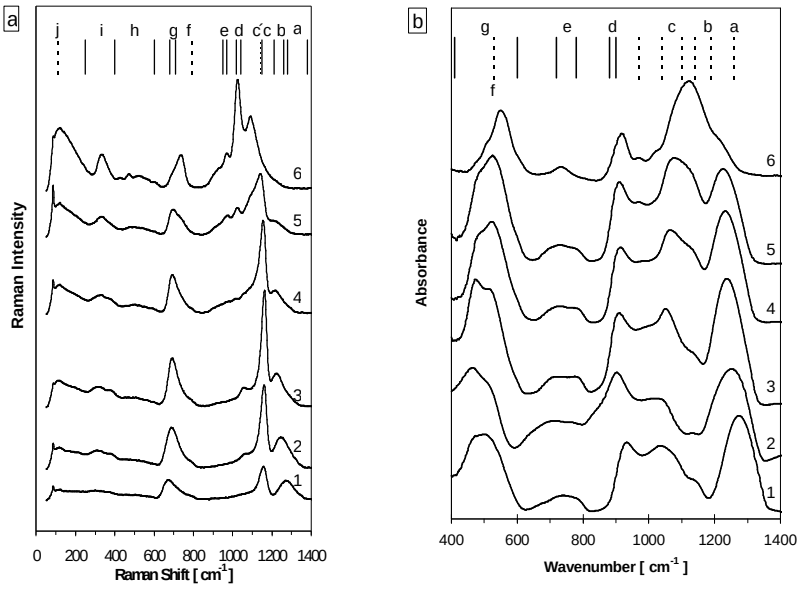

Fig. 1. The Raman a and infrared b spectra of glasses xPbO-10ZnO– (90-x)P_2O_5. The numbers mark the chemical composition, the small letters, the upper part of spectra, mark the frequency region, see Tables 1-3.

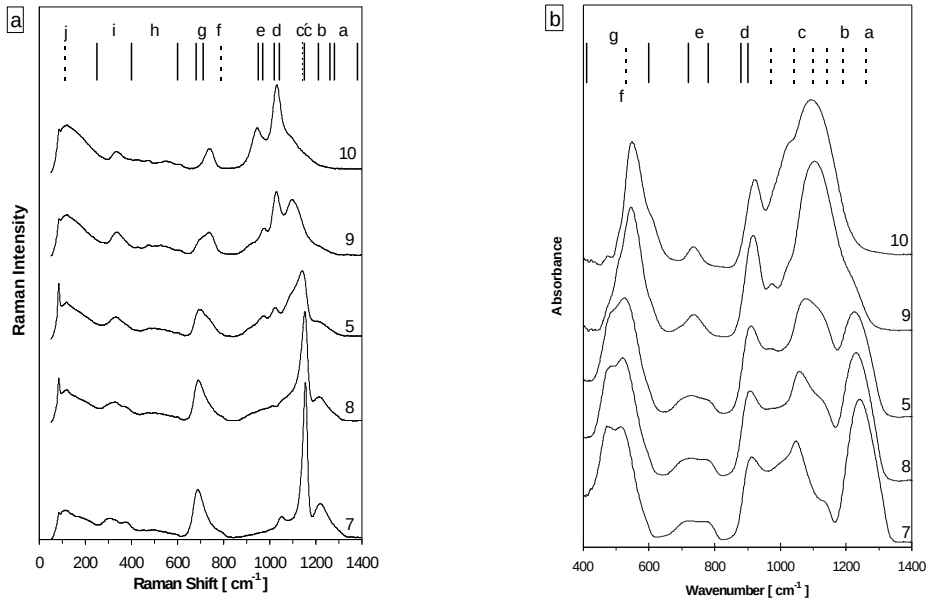

Fig. 2. The Raman a and infrared b spectra of glasses 50PbO-xZnO–(50-x)P_2O_5 . The numbers mark the chemical composition, the small letters, the upper part of spectra, mark the frequency region, see Tables 1-3.

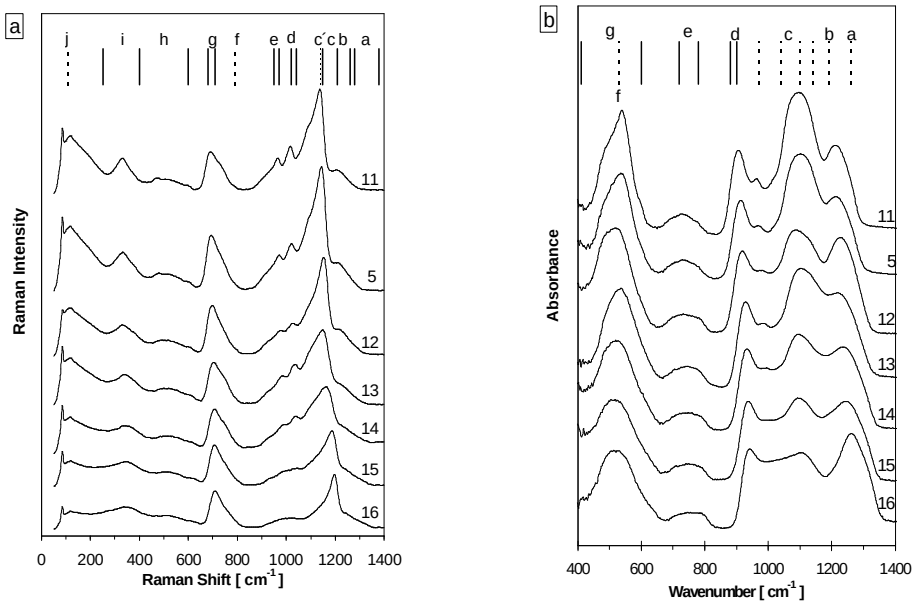

Fig. 3. The Raman a and infrared b spectra of glasses xPbO- (60–x)ZnO-40 P_2O_5. The numbers mark the chemical composition, the small letters, in the upper part of spectra, mark the frequency region, see Tables 1-3.

The Raman (RF) and infrared features (IRF) observed in phosphate glasses inclusive our glasses (Figs. 1a,b; 2a,b; 3a,b;) and their assignments are summarized in Tables 2(RF) and 3(IRF).

Table 2. The Raman features frequently observed in phosphate glassy systems and their assignment.

	Frequency [cm^{-1}]	Assignment and relevant references, e.g.
a	~ 1280-1380	(P=O) stretch mode, Q^3 units, [8,9]
b	~ 1210–1260	$(PO_2)_{as}$ stretch, Q^2 units, [2, 5, 9]
c	~ 1150-1210	$(PO_2)_s$ stretch, Q^2 units, [2, 5]
c´	~ 1140	$(P\text{-}O)^-$ stretch, Q^1 end groups, [2, 5, 9]
d	~ 1020-1040	$(PO_3)_{as}$ end groups, Q^1 units , the indication of $(P_2O_7)^{4-}$,[2, 10]
e	~ 950-970	PO_4^{3-} stretch, Q^0 units, [2, 5, 10]
f	~790	$(P\text{-}O\text{-}P)_s$ stretch in very short phosphate chains or in ring structure, [2, 11]
g	~ 680-710	$(P\text{-}O\text{-}P)_s$ stretch, Q^2 units [2, 12]
h	~ 400-600	bend mode of phosphate polyhedra and/or Pb-O, Zn-O vibrations, [2]
I	~ 250-400 (336)	PbO_4 tetragonal pyramid, [13-15]
j	~ 110	Pb-O more ionic bond, [14, 15]

Table 3. The IR features frequently observed in phosphate glasses and their assignment.

	Frequency [cm^{-1}]	Assignment and relevant references, e.g.
a	~ 1260	vibration mode P=O superposed with $(PO_2)_{as}$ mode in Q^2 units, [3,9,17]
b	~ 1190	$(P\text{-}O^-)$ vibration in Q^2 units, [3,18]
c	~ 1100-1140	broad band assigned to $(P\text{-}O^-)_{as}$ vibration in Q^2 units and/or (P-O-Pb) and/or (P-O-Zn) linkages [3,20]
	~ 1040	vibration of Q^0 tetrahedra [2, 5, 10]
	~ 970	$(P\text{-}O^-)_s$ vibration in Q^1 units [3, 18]
d	~ 880-900	$(P\text{-}O\text{-}P)_{as}$ vibration of BOs in linkages, [3, 17,19]
e	~ 720-780	$(P\text{-}O\text{-}P)_s$ vibration of BOs in linkages, [3, 17, 19]
f	~ 530	deformation mode of $P\text{-}O^-$ groups, [16]
g	~ 400-600	probably, also Zn-O tetrahedral bonds indication, [3, 20]

4. Discussion

4.1. Structural considerations

Before discussion of our results we shall briefly recapitulate some current ideas related to the structure of phosphate glasses, see e.g. [10]. The structure of phosphate glasses is mainly determined by the formal content of P_2O_5 ($[P_2O_5]$) and by the way how the PO_4 tetrahedra are interconnected.

In ultraphosphate glasses ($[P_2O_5]$ > 50 mol%), the structural types of units are $Q^{3,*}$ and $Q^{2,**}$ tetrahedra. The Q^3 units form three-dimensional network, while Q^2 units assist the chain formation. With a decrease in P_2O_5 content up to $[P_2O_5]$ = 50 mol %, the structure of phosphate network approaches to metaphosphates, and the network is based mainly on Q^2 units. Hence, the chains formed by – $(P\text{–}O\text{-}P)_n$ – bridges, and rings formed by Q^2 units, have formed the overall metaphosphate network. Only few chain-ends are formed by $Q^{1,***}$ units. The part of Q^2 units often called PO_2^- unit has two non-bridging oxygens, which are usually assumed to be different since the first terminal oxygen is bonded by double bond (P=O) while the other terminal oxygen forms $P\text{-}O^-$ bond. As pointed recently by Brow [10] there are, however, indications that both terminal oxygens in PO_2^- unit of Q^2 tetrahedra are indistinguishable because of the resonant bonds formation that is the

* The Q^3 units have three bridging oxygens (BOs) and one non-bridging oxygen (NBO) bonded to the phosphorus atom by a double bond [2,10];
** The Q^2 units have two bridging and two non-bridging oxygens (metaphosphate structure [10])
*** The Q^1 units have one bridging and three non-bridging oxygens (polyphosphate structure[10])

negative charge is almost equally delocalised over both the non-bridging oxygens in the Q^2 unit. Further decrease in the P_2O_5 content, i.e. $[P_2O_5] < 50$ mol %, leads to formation of polyphosphate glasses. Network of them is in fact depolymerised metaphosphate network formed by shorter chains of Q^2 units which are terminated by Q^1 units and, hence, $[Q^1]_{polyphosphate} > [Q^1]_{metaphosphate}$. For the content of $P_2O_5 \approx 33$ mol %, the structure of phosphate network is formed mainly by dimmers of Q^1 units, and for $[P_2O_5] < 33$ mol %, there exist mainly isolated $Q^{0,****}$ units. The transition from one type of Q^n units to the other type of units depends on the actual chemical composition of the melt, i.e. on the formal content of P_2O_5, and on the content and properties of the other participating oxides (network former and/or network modifier). Formally, this transition can be expressed by following relations:
$2\ Q^3 \leftrightarrow\ Q^2 + Q^1$ and $2\ Q^2 \leftrightarrow Q^1 + Q^0$, resp. Consequently, except of the main structural types Q^n, in each type of a glassy phosphate composition there can be present also some Q^{n-1} and also Q^{n-2} types of tetrahedra.

Raman spectra for the A-, B-, C- series of glasses, see Figs. 1a, 2a, 3a, indicate some similarities in the spectral regions around $\nu \sim 680$-710 cm^{-1} (RF_g), and $\nu \sim 400$ cm^{-1} (RF_h). We suppose, see Table 2 that an increase in the RF_h intensity with an increase in PbO content indicates that at higher PbO content a significant part of PbO is incorporated into a glass network as PbO_4 tetragonal pyramids. The persistence of RF_g at ~ 680-710 cm^{-1} indicates that independently on the chemical composition in all glasses studied the chains are present which, however, should have different distribution in the length. Comparison of the ratio of the most intensive RF_c in the region $\nu \sim 940 - 1380$ cm^{-1} to intensity of RF_g, indicate that the overall density of chains decreases with a decrease of P_2O_5 content in glasses of the series A, B, and with an increase in PbO content in the case of C-series glasses. The asymmetry in the high frequency side of RF_g indicates that most probably shorter chains are formed [2], that are this RF_g considered is an envelope of $RF_{f,g}$, see Table 2. The relevant part of IR spectra the IRF_e around $\nu \sim 720$-780 cm^{-1}, assigned to symmetric stretch mode of P–O–P linkages, see Table 3, is in harmony with RF_g. Similarly, as in the case RF_g, the asymmetry of IRF_e indicates some distribution in the chain length. The IRF_d around $\nu \sim 880$-900 cm^{-1}, assigned to asymmetric stretching mode of the P–O–P linkages persists in all compositions studied and its relative intensity is changing similarly to relative intensity changes of RF_e. It is clear indication of the presence of phosphate chains, which contain some distribution in a number of Q^2 units forming the chains. The assignment of the $IRF_{f,g}$ observed at ~ 400-600 cm^{-1} in all studied glasses is not unambiguous. As evident from the shape of this IRF it is composed from two and/or three bands which we tentatively assign, see Table 3, to IRF_f, deformation mode of $P–O^-$ groups. The IRF_g indicates the presence of Zn–O tetrahedral bonds, and most probably also the presence of PbO_4 structural units, which judging from the Raman spectra one can expect for high content of PbO also somewhere in the region $\nu \sim 400$–500 cm^{-1}, see e.g. [20].

4.1.1. The series A, x PbO - 10 ZnO – (90-x) P_2O_5, Figs. 1a, 1b

The dramatic changes in both the Raman and infrared spectra, following the chemical composition changes, are seen in the region ~ 940–1380 cm^{-1} that is in the region related to non–bridging oxygen modes. In the series A, Figs. 1a, 1b, the broad feature around 1270 cm^{-1} we tentatively attribute to overlap of RF_a and RF_b, see Table 2, that is to presence of some non–bridging P=O bonds in PO_4 tetrahedra only (in a few Q^3 units) but also to asymmetric stretch mode of PO_2 units in PO_4 tetrahedra. This last one is well seen in infrared spectra as IRF_a, see Fig. 1b, and the Table 3. An increase in PbO content and simultaneous decrease in P_2O_5 content leads to a decrease in the relative intensity of RF_a at ~ 1270 cm^{-1} which is also shifted towards lower frequencies. It is an indication of phosphate network depolymerization and most probably also formation rather resonant bonds in PO_2 units that is some decrease in the average bond number, see e.g. [21, 22]. The RF_c at ~ 1170 cm^{-1} corresponding to symmetric stretch mode of PO_2 units in PO_4 tetrahedra remains to be most important RF_c in the region $30 \leq x$ (mol %PbO) ≤ 50. However, as PbO content increases the RF_c is moving to lower frequency. When x reaches up the value $x = 50$, the RF_c is broadened on

**** Q^0 unit has four non-bridging oxygens (orthophosphates [10])

the low frequency side and the new features RF_d (x = 35, x = 40) and RF_e (x = 45, x = 50), appear. It is clear indication of further depolymerization of phosphate network by formation of PO_3-end groups (RF_d) and also formation of tetra– and triphosphate units. Finally, for x = 55, the dominant RF_d at ~ 1020 cm^{-1} and also well pronounced RF_e at ~ 950 cm^{-1} indicate that network is formed by a mixture of diphosphates, tri- and tetra-phosphates (RF_d) with a considerable number of PO_3 end groups ($RF_{d,e}$ ~ 1020, ~ 950 cm^{-1}). Consequently, an increase in PbO for P_2O_5 content, leads to transition from nearly ultraphosphate to metaphosphate network, and finally to pyrophosphate/orthophosphate ones.

Hence, the phosphate network is depolymerized but owing to the role of PbO as network former, the PO_2 units interact with PbO forming P–O–Pb linkages/bridges, which interconnect the chains together. Overall connectivity of the network increases, as documented by an increase in T_g, see Table 1 and Fig. 4. We suppose that ZnO, see e.g. [14] remains mainly to be bonded to PO_3–end groups. In agreement with this picture the IRF_c becomes to be dominant infrared response for high content of PbO (x = 55). Broadening of this feature, which one is related to symmetric stretching $P–O^-$ (phosphorus non–bridging portion of PO_4 tetrahedra in a chain structure that is in Q^2 units), indicates dispersion in the number of Q^2 units in the chains forming the phosphate network.

4.1.2. The series B, 50PbO–xZnO–(50 – x)P_2O_5, Figs. 2a, 2b

Starting from x = 0, the studied glasses represent the typical metaphosphate system with dominant RF_c due to symmetric stretching of PO_2 units within PO_4 tetrahedra, and two much less intensive features RF_b and RF_d related to asymmetric stretch mode of PO_2 in PO_4 tetrahedra and to symmetric stretch mode of PO_3-end groups, resp. Similarly, as in the case of series A, a decrease in P_2O_5 content, here substitution of ZnO for P_2O_5, leads to a network depolymerization as indicated by a broadening of RF_c at x = 10. The structure of the low frequency broadening part of RF_c indicates the presence of tetra- and tri-phosphates (RF_d, RF_e), and finally for x = 20, the formation of pyrophosphate units (RF_d, ν ~ 1020 cm^{-1}) and asymmetric stretch mode of PO_3-end groups (RF_e, ~ 950 cm^{-1}) are found, hence, the phosphate network is depolymerised. In harmony with changes found in Raman spectra the IR spectra indicate a decrease in PO_2 stretch mode (IRF_a, ~ 1250 cm^{-1}) and the considerable increase in IRF_c due to symmetric stretching motion of non-bridging oxygen atoms in Q^2 phosphate tetrahedra. We suppose that approximately in the region $0 \leq$ x(mol %ZnO) $\leq$ 10–15, ZnO behaves mainly like the network modifier [10], and it enhances the role of some fraction of PbO as a network former too, see e.g. [3]. With an increase in content of ZnO for P_2O_5 (x > 10–15), ZnO probably enters more into the network; it behaves like a network–former, "a competitor" to PbO. Consequently, such a network could be more cross-linked and hence, the glass-transition temperature increases with the ZnO content increase, see Table 1.

4.1.3. Series C, xPbO- (60 - x)ZnO - 40P_2O_5, Figs. 3a, 3b

The Raman spectra confirm that the network of studied glasses is built from the chains mainly; the RF_c (~ 1100 cm^{-1}) is dominant. The shape of this feature is, however, changing with the substitution of ZnO by PbO. With an increase in PbO content the low frequency asymmetry of this band is more pronounced, and two separated features are seen, namely RF_d (~1020 cm^{-1}) indicating formation of pyrophosphate groups, and RF_e (~ 950 cm^{-1}, due to asymmetric stretch mode of PO_3-end groups (Q^0 units)). Simultaneously, in the FTIR spectra (Fig. 3b), the relative intensity of IRF_a (~ 1260 cm^{-1}) decreases while the relative intensity of IRF_c (symmetric stretch of non-bonding oxygens in Q^2 unit) increases. Such a behaviour of both the Raman and the infrared spectra, indicate that increase in PbO for ZnO, at constant P_2O_5 content, leads to an increase in disorder of a network also due to an increase in network depolymerization and the length of virgin Q^2 chains decreases. Moreover, the Pb^{II} does not crosslink significantly the short phosphate chains. This seems to be in agreement with recent results [5]. Consequently, the increase in PbO content leads to a decrease in the glass transition/softening temperature, see Table 1, and see also [5].

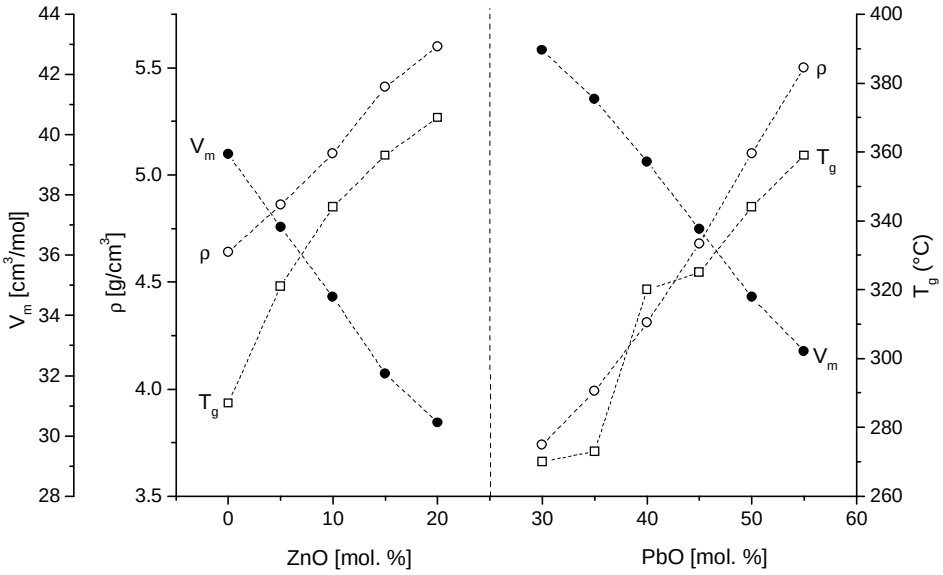

Fig. 4. The variation of the density (o), the molar volume (•), the glass transition temperature (□), of glasses 50PbO-xZnO–(50-x)P_2O_5 (left hand side) and of glasses xPbO-10ZnO–(90-x)P_2O_5 (right hand side). The dashed lines are only guides for the eyes.

4.1.4. Reflection of the phosphate network depolymerization into the other properties studied

In Fig. 4 the compositional dependencies of the density (ρ) and the molar volume (V_m), together with the glass-transition temperature (T_g), for glasses in which P_2O_5 is substituted by ZnO or PbO, are summarized for the reader´s convenience. An overall compositional trend of the dependencies in Fig. 4 is similar, that is with a decrease in P_2O_5, the density of glasses increase, followed by increase of the values of T_g while the values of V_m decrease. The decrease in V_m accompanied by an increase in T_g reflects most probably an overall increase in the glassy matrix cross-linking (compactness) as indicated by structural changes found in both the Raman and infrared spectroscopy, see parts 4.1.1 and 4.1.2.

Of interest are the compositional dependencies of all the V_m, T_g, and ρ quantities in the C series of studied glasses, see Fig. 5. There seems to be an indication of some jump-like changes in dependencies of V_m, versus [PbO] around the content of [PbO] = 40 mol %. At this content of PbO the T_g values drops down reaching at [PbO] = 40 mol % the minimum value of T_g = 329 °C. We suppose, that the decrease in T_g values reflects an increase in disorder of a network and an increase in network depolymerization as deduced from the results of both the Raman and infrared spectroscopy, part 4.1.3. We speculate that a local minimum seen in T_g(PbO) dependence at around [PbO] = 40 mol% could reflect a tendency of the system to some nano-phase separation. As pointed e.g. by Boolchand [23] nano-phase separation leads to a decrease in overall network connectivity which results into a decrease in T_g values. From the both the Raman and infrared spectroscopy the presence of both the metaphosphate units and diphosphate units were found, see part 4.1.3. As it is known that ZnO interacts preferably with PO_3-end groups, we speculate that following local nano-scale decomposition of a part of the network can not be excluded: $(PbO)_{40}(ZnO)_{20}(P_2O_5)_{40} \rightarrow 20\ Pb_2P_2O_7 + 20\ Zn(PO_3)_2$. Consequently, at [PbO] = 40 mol% the network connectivity could be significantly reduced by such a local decomposition, the network could be strained and, hence T_g drops down. With an increase in the PbO content on nano-scale separated entities of $Pb_2P_2O_7$ and $Zn(PO_3)_2$ could interact together forming entities of e.g. $(Pb_{5/6}Zn_{1/6})_3P_4O_{13}$). We note that Young et al. [24] in their study of crystallization kinetics of PbO-ZnO-P_2O_5 found formation of $(Pb_{5/6}Zn_{1/6})_3P_4O_{13}$ induced by annealing of $(PbO)_{50}(ZnO)_{10}(P_2O_5)_{40}$ glass. Overall compositional

trend of the step-like decreasing glass-transition and increasing molar volume follows both an increase in the density and an increase in overall polarizability of the network accompanied by an increase in the PbO content [25]. Jump like compositional dependencies in the optical properties (e.g. refractive index, optical gap) we also observed, see [25], associated with the structural changes also, we supposed.

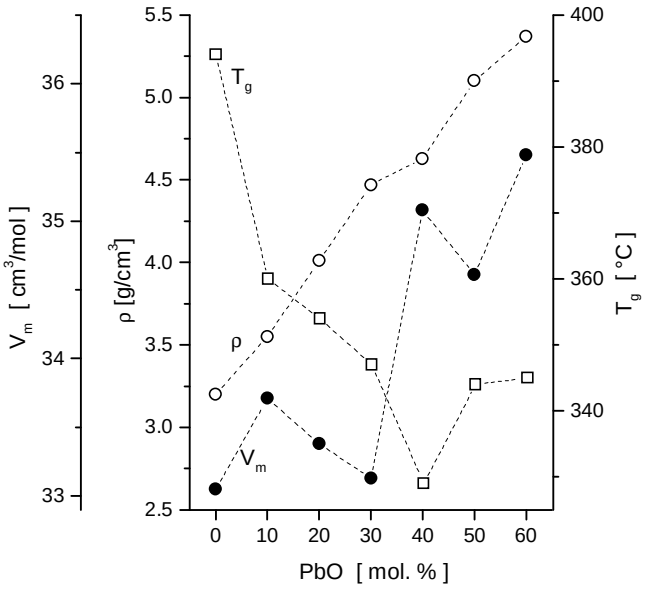

Fig. 5. The variation of the density (o), the molar volume (•), the glass transition temperature (□), of glasses xPbO-(60–x)ZnO-40 P_2O_5. The dashed lines are only guides for the eyes.

5. Conclusions

Three series of colourless PbO-ZnO-P_2O_5 glasses were prepared. The density of glasses increases with the increase in PbO content and, e.g. for C-series of glasses a change in the slope ρ(PbO) dependence at ~ 30-40 mol % PbO is evident indicating some structure changes in this region of PbO content. Results from the Raman and infrared spectroscopies are consistent with results mentioned above. The chemical composition of the glasses studied covers structural richness of phosphate glasses from ultraphosphate up to polyphosphate glasses. Both Raman and infrared spectra unambiguously indicate that the substitution of P_2O_5 by the both PbO or ZnO leads to a network fragmentation and depolymerization, but due to formation of P-O-Pb(Zn) linkages the network is more crosslinked which is for example accompanied by an increase in the glass-transition temperature. For a constant content of P_2O_5 the substitution of ZnO by PbO leads to an increase in the network disorder. At the chemical composition close to $(PbO)_{40}(ZnO)_{20}(P_2O_5)_{40}$ where the clear minimum in T_g(PbO) dependence is observed we speculate that some nano-phase separation could be responsible for a decrease in the overall network connectivity.

Acknowledgements

We acknowledge the support from the research project VZ 253100001 of the Czech Ministry of Education. L.T. acknowledges also support from the Key project ASCR 2050602 and from FWO Vlaanderen (Belgium).

References

[1] B. C. Sales, L. A. Boatner, J. Non-Cryst.Solids **79,** 33 (1986).
[2] H. S. Liu, T. S. Chin, Phys. Chem. Glasses **38**(No 3), 123 (1997).
[3] H. S. Liu, T. S. Chin, S. W. Yung, Mater. Chem. Phys. **50,** 1 (1997).
[4] H. S. Liu, P. Y. Shih, T. S. Chin, Phys. Chem. Glasses **37,** 227 (1996).
[5] G. L. Saout, F. Fayon, C. Bessada, P. Simon, A. Blion, Y. Vaills, J. Non-Cryst. Solids **293/295,** 657 (2001).
[6] M. D. Shcheglova, V. A. Yalanskaya, A. N. Kuznichenko, Khim. Tekhnol. (in Russian, Kharkov, USSR) **22,** 125 (1971).
[7] J. R. Van Wazer, Phosphorus and its Compounds, Vol. **1**, Interscience, New York, 1958.
[8] A. Mierzejewski, G. A. Saunders, H. A. A. Sidek, B. Bridge, J. Non-Cryst. Solids **104,** 323 (1988).
[9] K. Meyer, J. Non-Cryst. Solids **209**, 227 (1997).
[10] R. K. Brow, J. Non-Cryst. Solids **263-264,** 1 (2001); ibid **191,** 45 (1995).
[11] J. E. Pemberton, L. Latifzadeh, Chem. Mater. **3**, 195 (1995).
[12] Y. Jin, D. Jiang, X. Chen, B. Bian, X. Huang, J. Non-Cryst. Solids **80**, 147 (1986).
[13] D. Donaldson, M.T. Donaghue, S. D. Ross, Spectrochim. Acta A **30**, 1967 (1975).
[14] T. Furukawa, S. A. Brawer, W. B. White, J. Mater. Sci. **13**, 268 (1978).
[15] K. El. Egili, H. Doweidar, Y. M. Moustafa, I. Abbas, Physica B (2003).
[16] D. E. Corbridge, J. Appl. Chem. **6**, 456 (1956).
[17] M. Abid, M. Et-Sabiron, M. Taibi, Mater. Sci. Eng. B **97**, 20 (2003).
[18] R. F. Bartolomeew, J. Non-Cryst. Solids **7**, 221 (1972).
[19] J. O. Bynn, B. H. Kim, K. S. Hong, H. J. Young, S. W. Lee, A. A. Izyneew, J. Non-Cryst. Solids **190**, 288 (1995).
[20] J. C. Hurt, C. J. Phillips, J. Am. Ceram. Soc. **53**, 269 (1970).
[21] S. W. Martin, Eur. J. Solid State Inorg. Chem. **28,** 163 (1991).
[22] P. Subbalakshmi, N. Veeraiah, Mater. Letters **56,** 880 (2002).
[23] P. Boolchand, D. G. Georgiev, T. Qu, F. Wang, L. Cai, S. Chakravarty, Comptes Rendus. Chim. **5**, 713 (2002).
[24] S. W. Young, P. Y. Shih, T. S. Chin, Mater. Chem. Phys. **57**, 111 (1998).
[25] H. Tichá, J. Schwarz, L. Tichý, R. Mertens, J. Optoelectron. Adv. Mater. **6**(3), 747 (2004).